Conceptual design and numerical validation of a composite monocoque solar passenger vehicle chassis

Denny, Jason; Veale, Kirsty; Adali, Sarp; Leverone, Fiona

DOI
10.1016/j.jestch.2018.07.014

Publication date
2018

Document Version
Final published version

Published in
Engineering Science and Technology, an International Journal

Engineering Science and Technology, an International Journal 21 (2018) 1067–1077

HOSTED BY

Contents lists available at ScienceDirect

Engineering Science and Technology, an International Journal

journal homepage: www.elsevier.com/locate/jestch

Full Length Article

Conceptual design and numerical validation of a composite monocoque solar passenger vehicle chassis

Jason Denny [a,*], Kirsty Veale [a], Sarp Adali [a], Fiona Leverone [b]

[a] University of KwaZulu-Natal, 1 King Goerge V Avenue, Durban 4041, South Africa
[b] TU Delft, Kluyverweg 1, 2629 HS Delft, Netherlands

ARTICLE INFO

Article history:
Received 10 January 2018
Revised 17 July 2018
Accepted 19 July 2018
Available online 29 July 2018

Keywords:
Finite element analysis
Carbon fiber reinforced polymer
Monocoque chassis design
Composite structures

ABSTRACT

The concept of the composite monocoque chassis has been implemented in many vehicle designs; however, there is limited open literature defining the process of simulating a composite monocoque chassis. The purpose of this research is to develop a composite monocoque chassis by analysing its structural integrity through an iterative finite element analysis process with the intention of developing a lightweight solar-powered vehicle. Factors that influence this methodology include; the definition of the vehicle loading conditions, failure criteria, and important design parameters, chief among which is the torsional stiffness. The primary design criterion considered is the torsional stiffness which is determined from the application requirements and data available in the literature. The design methodology then follows an iterative process where various geometry and lay-up changes are considered. Under the same loading conditions, with the aim of increasing the torsional stiffness to achieve the required parameter. The ultimate strength of the material was also considered throughout the simulation process however, in most cases, the model failed to meet the torsional stiffness parameter before the material failure or delamination. Secondly, an analysis of the mounting points was conducted to ensure that the chassis is able to withstand the concentrated loads at the suspension mounts. This analysis is concerned with the principal stresses which gives insight into the most suitable orientation of the lay-up. The methodology presented in this paper stands to be supportive in designing a fully composite monocoque chassis for lightweight race vehicle applications.

1. Introduction

A monocoque chassis is a single piece structure with the body acting as a load-bearing member. It supports the suspension system, steering system, drive system, and other components. Effective chassis performance depends on maintaining rigidity in bending and torsion, providing efficient load absorption and reducing the overall weight of the chassis [1]. The objective of the present work is to develop a method for analyzing a composite monocoque chassis under operating conditions and to determine a structurally sound monocoque chassis through finite element analysis. The primary aim is thus to determine the feasibility of a fully composite monocoque chassis of a four-wheeled, lightweight, efficient solar-powered passenger vehicle. Complexities involved in this specific type of analysis include determining composite lay-up orientation, smart geometries for structural enhancement, and general motor vehicle safety requirements. Traditionally, due to their monocoque design, composite materials, are the materials of choice for the manufacture of solar vehicles [2]. Regarding chassis design, rigidity resistance and low weight, for handling performance, are the most important design parameters [3]. Since the vehicle is intended for solar power applications, it must be able to accommodate an appropriate solar panel array. The chassis design specifications, such as geometry constraints, were developed from the 2017 World Solar Challenge cruiser class rules and regulations [4]. The suspension mounting locations must be considered when designing a chassis. Designing a perfect suspension system for the application after the chassis has been designed could cause design complications. Consideration of the suspension systems helps depict the chassis geometry and space requirements at the wheel shrouds and mounting points [5]. A double wishbone system was selected for the front suspension due to its high handling performance and compact design [6,7]. This design has also been used extensively in other solar car designs. A trailing arm system was selected for the rear suspension due to its uncomplicated design and how well it fits into the

* Corresponding author.
E-mail address: dendog8117@gmail.com (J. Denny).
Peer review under responsibility of Karabuk University.

https://doi.org/10.1016/j.jestch.2018.07.014
2215-0986/

aerodynamic fairing [6]. Solar team *Nuon* has experienced remarkable success with *Nuna 8*'s double wishbone front suspension and trailing arm rear suspension, winning the 2015 World Solar Challenge challenger class [8].

A monocoque offers low weight and high rigidity properties [2], which is favorable for solar car chassis design, however can be considerably more complex to manufacture. In a monocoque chassis the stress generated by the vehicle during motion is distributed throughout the structure, alleviating localized stresses [3]. The monocoque thus exhibits increased torsional stiffness and an ability to resist twisting compared to other chassis types [9]. The torsional stiffness parameter is of utmost importance regarding chassis design as it enables the front and rear suspension systems to act correctly with respect to each other. This largely affects the vehicle's handling ability, in particular, its ability to corner [10]. If a vehicle has insufficient torsional stiffness, it would twist when loaded accordingly, lifting one end of the vehicle and causing one wheel to lose traction [10].

The most common materials used in the production of a monocoque chassis are composites [11], in particular carbon fiber reinforced polymers (CFRP) and Kevlar, because they exhibit high stiffness and strength to weight ratio properties and can be formed to virtually any geometry [12]. However, there are some disadvantages, such as intricate design procedures, high cost and complex manufacturing processes [13]. CFRP monocoques offer among the highest stiffness to weight ratios, when compared to any material and chassis type combination [2]. This is the primary reason why carbon fiber composites are extensively used in solar car chassis design [14].

Existing monocoque solar vehicle chassis designs were investigated to gain an understanding of the shape and geometry features of effective designs. This knowledge was used to develop the preliminary chassis geometry, detailed in Section 7. Solar Team Eindhoven implemented a full CFRP monocoque in their 2015 World Solar Challenge vehicle, *Stella* Lux [15]. The chassis consisted of a dual-hulled, catamaran-like shroud with a tunnel underneath the chassis center, reducing the frontal area and improving the aerodynamics. Kogakuin University finished in second place at the 2015 World Solar Challenge with their solar-powered car, *OWL*. *OWL* which was constructed as a full monocoque using Teijin CFRP prepreg, resulting in the chassis weighing as little as 55 kg [16]. Consistent with *Stella Lux*, *OWL* has a large tunnel in the middle beneath the chassis to reduce its frontal area. The vehicle manufactured by University of New South *Wales*, called *Sunswift*, also exhibits this tunnel to reduce the frontal area [14].

2. Materials

Woven carbon fiber composite reinforcement materials are the materials of choice for solar vehicle monocoque chassis design [17]. They easily form complex shapes, are robust, have greater resistance to damage, and reduce lay-up time [18]. The woven structure of the alternating fiber directions are composed by warp and weft fibers which means that the structure exhibits mechanical properties in multiple directions, making it more suitable in solar vehicle chassis design. Depending on the type of weave, the woven structures exhibit diverse mechanical properties. The most common types of weave are plain, twill and satin. In the plain weave, each warp fiber passes alternatively under and over each weft fiber; this is the most stable weave to prevent strand slippage and distortion, but the high level of fiber crimp imparts relatively low mechanical properties compared to other weave styles. The long fiber sections in a satin weave result in better energy absorption and low fiber crimp, but reduced stability and increased likelyhood of fiber distortion. In a twill weave, one or more warp fibers alternatively weave over and under two or more weft fibers. A 2×2 or 4×4 twill offers the best compromise between the various conflicting factors that govern the choice of weave. In industry, the weave most commonly used is the 2×2 twill [18].

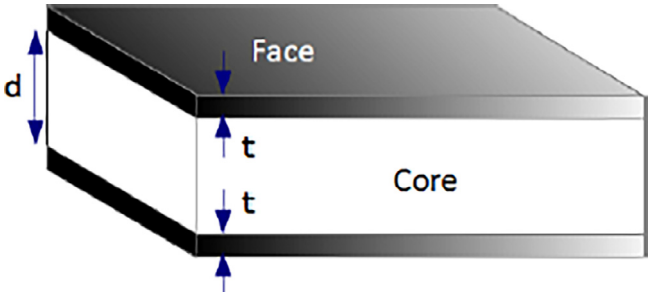

Fig. 1. Typical sandwich structure [19].

A woven fiber and a matrix material are generally combined with another material to form what is known as a sandwich structure – see Fig. 1 [19], which offers similar structural properties to an I-beam, but with overhangs and webs extended in all directions [20]. This additional material is called the core of the sandwich structure and is purposed to increase the rigidity of the structure since it acts similarly to an I-beam's web, which is favorable for chassis design. The core material is normally a low strength material, but its higher thickness, d, provides the structure with increased bending stiffness and overall low density. The core increases the moment of inertia and section modulus of the structure, resulting in better resistance to buckling and bending loads [21]. The face or skin material surrounds the core on its upper and lower sides and acts as the overhangs of the I-beam. When loaded in bending, one of the skin materials experiences tension and the other compression, and the core is loaded in shear, which offers rigidity and strength to the entire structure. The thickness of the face material, t, is small in comparison to the thickness of the core. Common core materials used in monocoque chassis construction include polyurethane foams and aluminum and Nomex honeycombs [2].

Composite sandwich structures have emerged as one of the most promising material options for many weight reduction applications, which is key in solar vehicle design. It yields improved fatigue performance, superior energy absorption, corrosion resistance, and weight reduction when compared to the individual materials used to construct the sandwich [21].

3. Failure criteria

Failure occurs when a structure can no longer perform its intended function and gives rise to the need for failure criteria to be defined when simulating a design. Composite failure criteria can be divided into two main groups, namely failure criteria not associated with failure modes and failure criteria associated with failure modes [22]. The first uses analytical expressions to describe the failure surface as a function of the material's mechanical properties, which are determined by fitting an expression to a standardized curve attained through experimental methods. Proposed by Tsai and Wu [23], the Tensor Polynomial Criterion is the general polynomial failure criterion used for composite materials and is expressed as:

$$F_i \cdot \sigma_i + F_{ij} \cdot \sigma_i \cdot \sigma_j + F_{ijk} \cdot \sigma_i \cdot \sigma_j \cdot \sigma_k \leqslant 1 \quad (1)$$

where $i, j, k = 1, 2, 3, 4, 5, 6$ for a three-dimensional case. The lamina strengths in the principal directions are given by the parameters F and lamina stresses in the principal direction are denoted as σ.

Generally, the third order parameters are neglected due to their complexity [23]. This yields Eq. (2):

$$F_i \cdot \sigma_i + F_{ij} \cdot \sigma_i \cdot \sigma_j \leqslant 1 \tag{2}$$

Furthermore, since the change of direction of shear stresses does not influence the material failure, all first-order shear stresses become negligible, i.e., *F4 = F5 = F6 = 0*. For orthotropic materials with three planes of symmetry orientated with the coordinate directions (namely the *i*, *j*, and *k* directions corresponding to the three-dimensional axes) and assuming *Fij = Fji* and that there is no coupling between the normal and shear stress terms, yields Eq. (3):

$$\begin{aligned} &F_1 \cdot \sigma_1 + F_2 \cdot \sigma_2 + F_3 \cdot \sigma_3 + 2F_{12} \cdot \sigma_1 \cdot \sigma_2 + 2F_{13} \cdot \sigma_1 \cdot \sigma_3 \\ &+ 2F_{23} \cdot \sigma_2 \cdot \sigma_3 + F_{11} \cdot {\sigma_1}^2 + F_{22} \cdot {\sigma_2}^2 + F_{33} \cdot {\sigma_3}^2 \\ &+ F_{44} \cdot {\sigma_4}^2 + F_{55} \cdot {\sigma_5}^2 + F_{66} \cdot {\sigma_6}^2 \leqslant 1 \end{aligned} \tag{3}$$

The second composite failure criterion adapts the empirical lamina composite failure criteria and is similar to the criteria used in the design of isotropic materials. It is more difficult to account for failure modes in a design with these criteria. Fiber fracture is a failure mode defined by the material's ultimate tensile strength and will not occur provided the maximum principal stress does not exceed the material's ultimate tensile strength in the direction of the stress.

4. Torsional stiffness

The torsional stiffness of a chassis is defined as its ability to resist twisting. It is considered one of the most important parameters to optimize in chassis design since it is largely responsible for the handling of a vehicle [24]. However, there comes a point when a chassis becomes sufficiently stiff and any further increase in the torsional stiffness would yield little if any, improvement to the chassis performance. Modern high-performance vehicles exhibit enormous torsional stiffness values because they generally have a large mass and travel at high speeds. This combination of a large mass and high-speed results in immense forces being exerted on the chassis, which requires an appropriate torsional stiffness value so that the chassis does not deform under the stress. For lightweight race vehicles, a lower torsional stiffness value is required. Small race vehicles commonly have torsional stiffness values of roughly 4000 Nm/deg [25], as opposed to that of a formula one car, which is 20,000 Nm/deg and higher [26]. Small race vehicles, such as solar vehicles, are not required to attain the high speeds of a formula one car, resulting in the vehicle being subjected to lower stresses. A solar vehicle competes in endurance racing in which efficiency is the key. The vehicle is only permitted to travel at highway speeds and will not be required to corner quickly. Only gradual highway curves and bends, which exert low forces on the suspension, need to be considered. This means that a solar vehicle does not require an exceptionally high torsional stiffness value, however, the chassis must withstand the increased stress exerted from encountering irregularities on the road such as potholes. A solar vehicle can be considered a small race vehicle for which a torsional stiffness ranging from 1000 to 4000 Nm/deg is sufficient [27].

The torsional stiffness of a chassis is difficult to obtain from a chassis' complex geometries without physical experimentation. However, through some simplifications and expanding on the principles of solid mechanics, a method for determining an approximate torsional stiffness can be developed. Assuming that the chassis can be modeled as a sequence of different cross-sections secured together and that the method of superposition applies to them, an expression for the overall torsional stiffness can be established by superimposing the individual stiffness values of the components [10]. Another assumption is that these cross-sections remain undistorted in their own plane because it is uncertain how the vehicle's geometry would react under torsional loading. This is a good approximation, but it does result in some inaccuracies [28]. These assumptions are applied to a finite element analysis model. To determine the torsional stiffness of a chassis the rear suspension mounts are constrained to be fixed in all directions, and equal, and opposite loads are applied to the front suspension arms [29]. This induces a torque on the chassis. The key parameter in this analysis is the deflection of the front suspension arms. The torsional stiffness (K_T) is given by [29]:

$$K_T = \frac{T}{\varphi} = \frac{FB}{\left(\varphi_p + \varphi_d\right) * 0.5} \tag{4}$$

where:

$$\varphi_d = tan^{-1}\left(\frac{v_d}{B/2}\right) \tag{5}$$

$$\varphi_p = tan^{-1}\left(\frac{v_p}{B/2}\right) \tag{6}$$

The force (*F*) is applied to the front suspension mounts and induces a torque (*T*) because of the perpendicular distance created by the wheel track (*B*). Eqs. (5) and (6) are used to determine the angular deflections, (φ_d) and (φ_p), of the driver and passenger sides of the vehicle by measuring the vertical deflections, (v_d) and (v_p), of the respective suspension arm ends. Since the chassis is symmetrical the driver and passenger side deflections are equal.

5. Weight

The weight of a chassis has a significant effect on the rolling resistance of the vehicle [12]. It is imperative that the weight be minimized without compromising the structural integrity of the vehicle. The forces exerted on the chassis from the suspension are proportional to the weight of the chassis [5]. Heavier vehicles have a greater tendency to remain on their intended path due to inertia when cornering, resulting in higher forces being transferred to the chassis when the tires oppose this to alter the vehicle's path. This increases the risk that the vehicle may experience understeer. Lower weight also results in improvement on the vehicle's acceleration and braking capability.

6. Finite element analysis

A monocoque chassis is inherently difficult to analyze accurately using analytical methods due to the complexity of the structure. It requires a complex mathematical model to describe it and simplifications would reduce the accuracy of the results [30]. A computational method of solution, which is fundamentally based on analytical methods, provides a powerful tool to obtain accurate results in the analysis of a monocoque chassis. Computational simulations are often used to obtain an approximate idea of how the design will react to operating loads before building a physical model and yields a means of determining the most suitable materials and geometry design for the application [31]. A finite element analysis can accurately simulate the loads experienced by a chassis in a shorter period than the appropriate numerical solution. However, a simulation is still only a representation of the design's performance and does not necessarily reveal the influence of the loads by problem variables, such as material properties and geometric features, small geometric features influence the mesh seeding in a finite element analysis. User input data errors can also result in false confidence in questionable simulation results.

One of the most important key performance indicators regarding chassis design is the torsional stiffness parameter [32]. The torsional stiffness is largely responsible for the ability of a vehicle to corner. A static cornering/torsional stiffness model is developed to verify how the chassis behaves while cornering and is able to quantify the design parameters that generate the requirement of torsional stiffness [2]. A previous static model by Milliken and Milliken's Race Car Vehicle Dynamics [1995] states that chassis stiffness can be designed to be approximately X times the total suspension roll stiffness, or X times the difference between the front and rear suspension stiffness. X generally ranges between 3 and 5 [26]. The torsional stiffness of a chassis determines how similar the roll angles of the front and rear suspension will be when cornering. A rigid chassis will force the rear suspension roll to be similar to that of the front. Different roll angles will result in lateral load transfer, affecting the handling of the vehicle. It must be noted that increasing the chassis torsional stiffness may increase the weight, particularly with an increase in core thickness and number of face material layers. A compromise must be made to ensure that a chassis with sufficient torsional stiffness and low weight characteristics is developed.

The complexity of a monocoque chassis makes it difficult to accurately simulate the torsional stiffness parameter. It is common to make geometry simplifications to simplify the model, decreasing the intricacy of the analysis. A previous method used in Hagan, Rappolt and Waldrop's Formula SAE Hybrid Carbon Fibre Monocoque/Steel Tube Frame Chassis [2014] to determine the torsional stiffness is to model the monocoque as a tube structure of diameter equal to the wheelbase of the vehicle [31]. One end of the tube is constrained to radial displacement while the other is subjected to a shear load of some predetermined magnitude. The problem with this model is that it is oversimplified and does not yield accurate results. This research aims to develop a method of modeling a monocoque chassis, without oversimplifying the model.

An iterative finite element analysis approach was used to optimize the structural integrity of the monocoque chassis. A linear static finite element analysis using Siemens NX Nastran [33] was conducted to obtain the simulation result. A preliminary model was developed from the knowledge gained by reviewing existing solar car designs [14–16] and UKZN solar car knowledge. Various advantageous chassis design techniques, such as reducing the frontal area, were adopted from the existing solar car designs and applied to the model geometry. Target parameters, including torsional stiffness, were developed from investigating chassis loading conditions, detailed in sub-section 6.2. The torsional loading case was used to develop a torsional stiffness model used in determining the chassis torsional stiffness. Composite failure criteria, detailed in Section 3, were used to determine a benchmark torsional stiffness value. To determine the torsional stiffness, the preliminary chassis model was modeled as a 2-D shell with CQUAD4 elements, by the layered-shell modeling technique, details of which are given in Section 7. The 2–D laminate elements, Fig. 2a, assume that each ply is in a state of plane stress, the plies are perfectly bonded, the transverse displacement and in-plane rotations are continuous, and shear deformation through the thickness of the laminate is constant. 1-D mesh collectors were used to represent the front suspension – see Fig. 2b. RBE2 elements, of negligible mass, represent the front suspension arms and transfer the wheel load to the chassis, without absorbing any of the stress.

The finite element analysis follows an iterative process where the torsional stiffness parameter is analyzed. The rear suspension mounts were fixed, as per the model instructions, and equal forces, detailed in sub-section 6.2, were applied to the front suspension arm ends, in opposite directions. This model creates a moment around the center of the vehicle, generating a means of determining the chassis' torsional stiffness. Geometry and layup modifications were applied to the model until a suitable torsional stiffness value was obtained. The purpose of the modifications is to alter the geometry and layup in strategic regions of the chassis with the intention of increasing the moment of area and thereby the torsional stiffness about the rotational axis of the torsional loads.

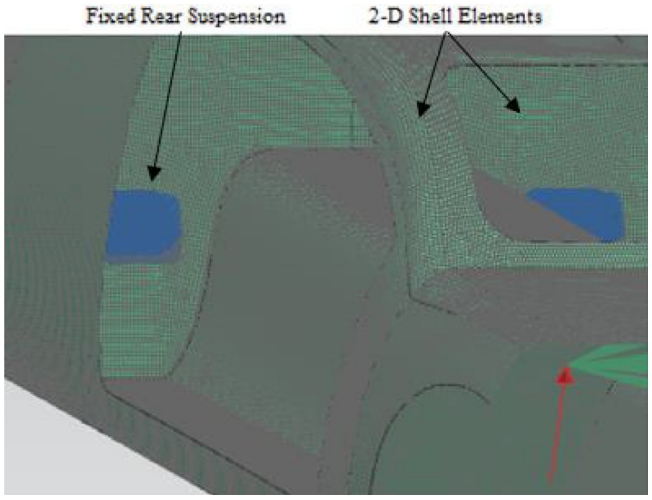

Fig. 2a. Rear suspension constraints.

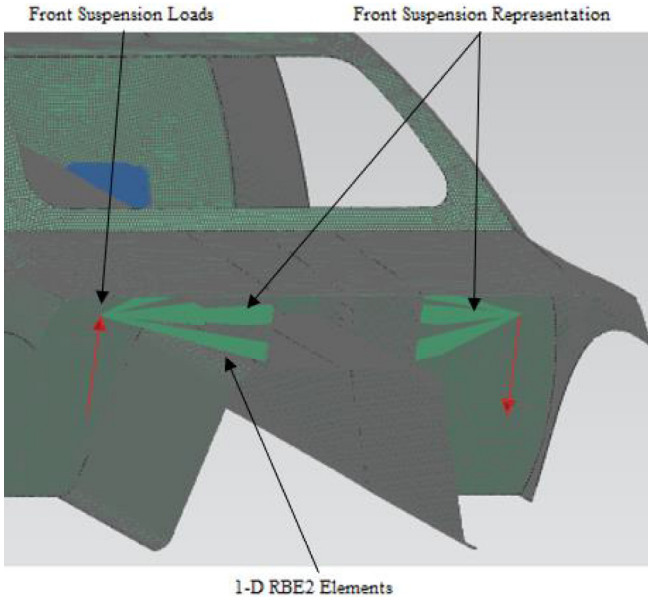

Fig. 2b. Front suspension load representation.

6.1. Modeling techniques

There are two main approaches when modeling a composite monocoque. The first is the 'shell-solid-shell' [34] which involves modeling the core material as homogenized three-dimensional solid elements and the face material as shell elements [35], connecting them by contact formulation. This approach yields a good representation of the possible core failure modes, but it is computationally rather expensive. The second is the 'layered shell' [34] approach which models the entire chassis as multi-layered shell elements and is a less computationally taxing method. Inside a one-shell element a number of sub-layers can be defined in the

thickness direction, representing the core and face laminate layers [34,35]. This method does not assess the possible core failure modes well but is considered sufficiently accurate when simulating chassis design parameters, such as torsional stiffness and principal stresses. Another approach used in modeling a composite monocoque is the 'stacked shell' approach [34]. This approach is similar to the 'layered shell' with the addition of an energy absorption mechanism and a degradation factor of the laminate's stiffness to account for interlamination delamination [34]. The main difference between the two is the main failure mode exhibited. In the 'layered shell' model interlamination failure in fiber tension mode occurs and in the "stacked shell" model interlamination failure in the delamination mode occurs [34]. Since the delamination failure mode is not being assessed in this work the 'layered shell' approach was selected as the modeling technique to be implemented.

6.2. Loading conditions

A vehicle's chassis is subjected to various loads whilst in operation, the bulk of which originates from the suspension. In the present study only normal operating loads are verified since thermal loads will be negligible; the chassis is intended for solar powered applications meaning that heat from an internal combustion engine is not present. The loading conditions on a chassis can be divided into global and local loading conditions. Global loading conditions are concerned with loads that the chassis is subjected to as a whole. These can be categorized as four main cases, namely, torsional loading, vertical bending, lateral bending, and horizontal lozenging. Torsional loads twist one end of the chassis with respect to the other and can arise from a variety of sources with the most common case being when a wheel contacts a bump raising that wheel in relation to the others – see Fig. 3 [36], which applies a torque to the chassis. The torsional stiffness parameter of a chassis is its ability to resist this twisting motion. A chassis without sufficient torsional stiffness would not be able to resist this torque, causing the vehicle to lose traction.

Vertical bending is the term given to the 'squatting' or 'diving' of the chassis when accelerating or decelerating. When accelerating the chassis 'squats' – see Fig. 4 [36]. When decelerating the chassis 'dives'. Because vertical bending does not affect the traction of a vehicle, it is considered a design parameter of less significance than torsional stiffness. In addition, a chassis with sufficient torsional stiffness will also have sufficient bending stiffness [26].

Lateral bending – see Fig. 5 [36], occurs as a result of the centrifugal forces that a chassis is subjected to whilst cornering. The vehicle's inertia induces a torque which is transferred to the chassis via the suspension, resulting is chassis roll [9]. This scenario is largely dependent on the weight and height of the vehicle. Chassis roll should be limited because it largely affects the stability of the vehicle, but does not affect stability as severely as the torsional stiffness.

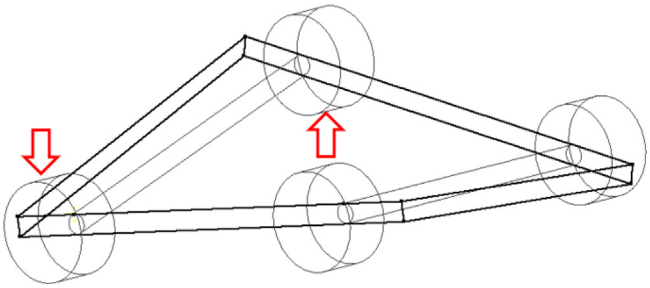

Fig. 3. Effect of torsional load on a chassis [36].

Horizontal lozenging – see Fig. 6 [36], is the response of a chassis when one side of the vehicle has better traction than the other. The unequal horizontal force distorts the chassis into a parallelogram-like shape. This scenario is considered of less

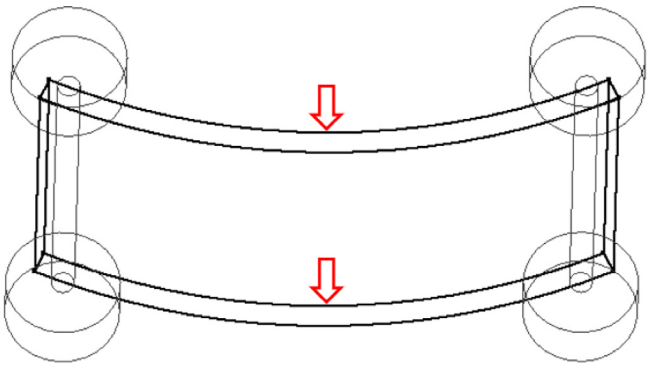

Fig. 4. Squatting effect due to acceleration [36].

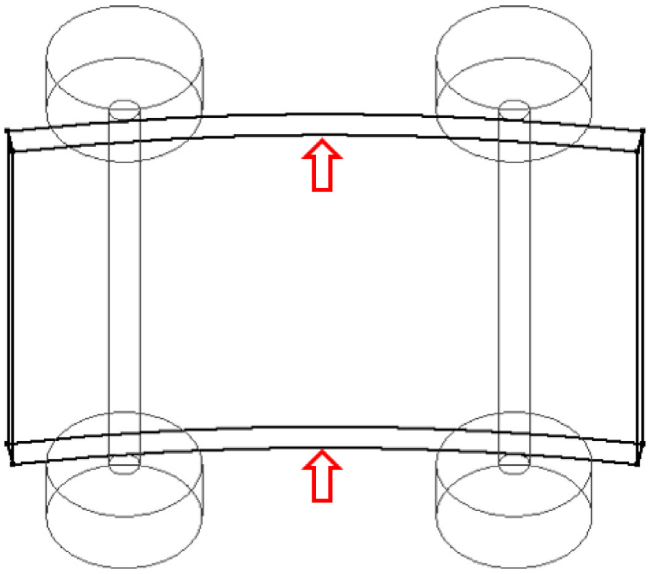

Fig. 5. Effect of lateral bending on a chassis [36].

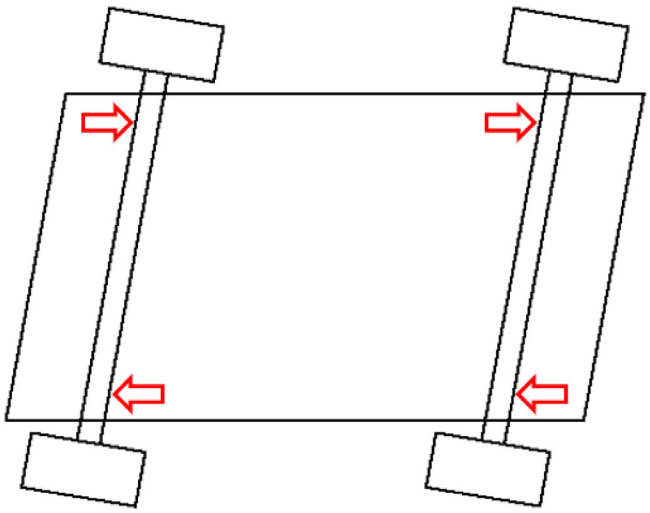

Fig. 6. Effect of horizontal lozenging on a chassis [36].

concern than torsional stiffness, vertical bending and lateral bending parameters of chassis design because it is more dependent on the traction of the tires than the chassis [37].

The torsional stiffness model is specified as the primary loading condition when simulating the design, and the lateral and vertical bending loading conditions are verified as secondary load cases. This would verify that a chassis with sufficient torsional stiffness exhibits sufficient bending stiffness. A summary of the constraints and loading conditions used for each load case is given in Appendix A. For the vertical bending analysis, the deflection ratio is of utmost importance [38]. For this analysis, the chassis is modeled as a simply supported beam, supported at the suspension mounts and the load applied to the chassis center. Beam theory suggests that the deflection ratio is defined as the ratio of the deflection of the center of the chassis to its length [38] and should be limited to 1/360th of the chassis length [39]. For the lateral bending analysis, the load is applied to the side of the vehicle, to simulate the lateral loads induced when cornering.

Local loading conditions are concerned with loads at mounting locations such as motor suspension mounts. These areas are subjected to high-stress concentrations as they are effectively the points where stress is transferred to the chassis. It is required that these mounting locations are sufficiently rigid and have adequate strength to withstand the concentrated loads present. A 'hardpoints' analysis is required to be conducted at these points. This involves analyzing the principal stresses at the mounting locations, and ensuring that the maximum principal stress does not exceed the ultimate tensile stress of the composite in the direction of the stress. This ensures that the failure mode of fiber fracture does not occur.

The load case and the magnitude of the applied loads for the simulation to determine the parameters of the chassis must be selected. Composite monocoques are unique in the way that they distribute the stresses from the suspension loads. They are designed in such a manner that the body itself experiences very little stress. This is due to the mounting points and inner structure absorbing the bulk of the applied stress. As previously mentioned, the torsional stiffness parameter is of utmost importance regarding the chassis design. To maximize the torsional stiffness of the chassis the most severe load case, being the bump case simulating the vehicle hitting a bump or pothole at speed, is required to be simulated. This load case transmits a vertical force through the suspension arms to the mounting points. The magnitude of this load is difficult to determine, but a conservative estimate is three times the weight experienced at the loaded wheel [17]. Since the weight of the vehicle is unknown, a good approximation of the weights of parts was defined. An assumption of masses of 40 kg for the chassis, 35 kg for the battery box, 10 kg for mechanical systems, and 5 kg for electronics was made from existing UKZN solar car knowledge [40] because a similar solar array and electronic configuration is to be implemented in the design of similar vehicles. The masses of the suspension systems, wheels, brakes, and motors are excluded in the analysis as these are unsprung masses which do not load the mounting points as they are attached below the shock absorber. As per the Bridgestone World Solar Challenge rules and regulations, the mass of each occupant must be a minimum of 80 kg. Accounting for two occupants yields a total sprung mass of 250 kg. Assuming that the vehicle weight is evenly distributed, each wheel should experience a weight of 62.5 kg (625 N). With the bump case exerting an acceleration of approximately 3 g [17], the force from the suspension will be 187.5 kg (1875 N) at each mounting location. To accommodate for any miscellaneous component weights, the 1875 N weight can be increased by ten percent, yielding a force of approximately 200 kg (2000 N). Although much greater than the assumed weight at each wheel, this force is a conservative approximate to ensure that failure in both yield and fatigue are avoided.

7. Finite element analysis results

A static model was developed to determine the torsional stiffness of the chassis from the torsional loading case mentioned in the loading conditions section because this case was deemed to be the worst-case scenario regarding loading conditions. This load case is used to determine the torsional stiffness parameter of the chassis. For the finite element analysis, *Siemens NX Nastran* [33] was the software used for the modeling of the chassis. Once a suitable geometry model was developed, a suitable mesh was generated for the simulation. For the model CQUAD4, two-dimensional shell elements were used to simulate the material with an average element size of 10 mm to compensate for varying changes in curvature. The element size was deemed adequate because the geometry is large in comparison to the element size, with a length of approximately 4500 mm and width of 1800 mm respectively, which ensures that the elements accurately represent the areas of high curvature exhibited by the geometry. A mesh independency study was conducted in which the average element size was reduced and yielded no significant variation in the simulation results, meaning that the 10 mm element size demonstrated adequate mesh independence. Siemen's NX Nastran offers an integrated element quality analysis tool that accounts for mesh quality checks, such as aspect ratio, and warpage and skew angle, on each element. Once run, the elements which do not satisfy the mesh quality threshold parameters are exposed. The mesh quality check resulted in some elements being moderately deformed but not sufficiently to affect the simulation results. In addition, these elements were located at non-critical areas, such as the wheel fairing, of the chassis and therefore did not affect the results. A bonding strength of 50 MPa between layers was specified for the laminate layers to simulate the bonding of the matrix material. This is the bonding strength as specified by the manufacturer, AMT Composites [41]. A 2×2 twill carbon fiber weave was selected as the skin material for the simulation because it offers a good compromise between the favorable properties of the plain and satin weave. A foam core was selected for the initial simulations due to its low density and high formability. The deflection result from the model of the driver and passenger sides of the chassis were substituted into Eqs. (5) and (6) respectively, along with the track width of the chassis, to obtain the angular deflection of the chassis. This angular deflection was then substituted into equation (4), along with the applied force and track width, to obtain the average torsional stiffness of the chassis. Various core and fiber material combinations were investigated until a suitable torsional stiffness value was obtained. An aluminum honeycomb exhibits superior stiffness properties when compared to a foam core and was also investigated to determine its effect on torsional stiffness.

The first step in analyzing the structural integrity, through a finite element analysis, of a composite monocoque chassis is to develop an initial model and lay-up procedure. This is determined by using existing UKZN solar car knowledge [40] and reviewing the relevant literature [30,31,42] on chassis design regarding geometry modeling techniques and laminate lay-up orientation. The next phase is to develop conceptual designs, using knowledge gained from relevant literature [15,16], adhering to the design specifications, and selecting the most suitable concept to be implemented as the final design. The design of a composite monocoque chassis is an iterative design process. Different geometry alterations and laminate lay-up orientations were investigated until the torsional

stiffness parameter was achieved. For the preliminary design shown in Fig. 7, the chassis was designed as a full monocoque that can accommodate two occupants. The vehicle is longitudinally symmetrical and constructed from smooth, gradual contours to minimize aerodynamic drag and stress concentrations. The roof and hood of the vehicle only curve in one direction to ensure that solar panels can be mounted efficiently. The cove that runs underneath the vehicle, to reduce its frontal area, has a constant area and gradual shape changes for aerodynamic purposes. The front and rear shroud geometries were designed to accommodate double wishbone and trailing arm suspension systems respectively.

An initial laminate lay-up was determined from the literature, specifically from the 2015 UKZN Solar Vehicle, *Hulamin* [43], and applied to the sections of the chassis as follows:

- Roof and Sides – [0°; 45°; 10 mm core; 45°; 0°]
- Suspension Mounts – [0°; 45°; 0°; 10 mm core; 0°; 45°; 0°]
- Inner Structure – [0°; 45°; 5 mm core; 45°; 0°]
- Front and Rear – [45°; 3 mm core; 0°]

A 2 × 2 twill carbon weave was selected for the laminate face material, along with a polyurethane foam core. The mechanical properties of the material are summarized in Appendix B [41]. Since a twill weave is used, only fiber orientations of 0° and 45° are used because 0° orientation is the same as 90° orientation, the same being the case for a 45° and −45° orientation. The warp fiber direction corresponds to the material orientation coordinate system and the weft fiber direction perpendicular to the warp fiber orientation. An aluminum honeycomb core is compared in this paper to the foam core to determine the effect on the torsional stiffness. A linear static simulation was created to record the reaction of the chassis to the loading conditions. The deflection, shown in Fig. 8, is used to determine the torsional stiffness of the chassis. Since the chassis is longitudinally symmetrical the deflections of the front left and right suspension ends are identical. Fig. 8 shows a deflection of approximately 5.373 mm at the front suspension ends, and when substituted into the relevant equations, along with a force of 2000 N and a track width of 1.3 m, through the above-mentioned calculation process, yields a torsional stiffness of 5489.8 Nm/deg which satisfies the failure criteria of 4000 Nm/deg. The estimated mass of the chassis is calculated by summing the individual solid property masses for each laminate section which yields a mass of 43.41 kg and validates the initial assumption of 40 kg for the chassis mass.

Although the required torsional stiffness value was achieved the effect of the geometry and lay-up modifications on the torsional stiffness were investigated.

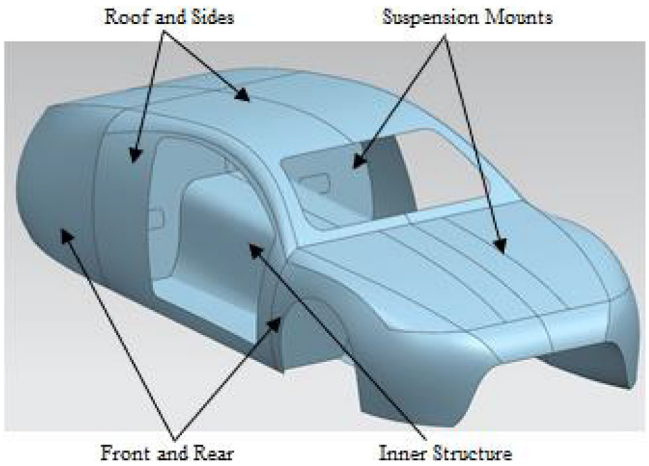

Fig. 7. Preliminary design model.

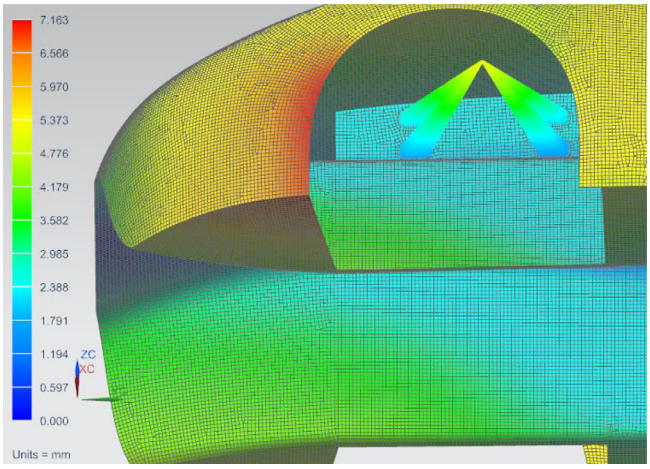

Fig. 8. Preliminary model front suspension deflection.

7.1. Design modifications

To reduce the mass of the chassis, sections of the chassis were altered based on the finite element results of the preliminary model. The finite element analysis illustrated that the deflection of the chassis decreases toward the rear. This is because the front and center of the chassis absorb most of the stress generated from the applied load and deflect accordingly. This implies that a geometry alteration in the rear region will have a negligible effect on the torsional stiffness. Sections were removed from the rear support plate and the rear suspension mount, as shown in Fig. 9 to reduce the mass of the chassis. Rear suspension access hatches were cut into the rear sides of the chassis, as shown in Fig. 9, to create access to the rear suspension components and to reduce weight.

It was observed that the large door recesses have a significant effect on the torsional stiffness. These large holes reduce the ability of the chassis to resist twisting. To test this theory, the door recesses were patched up and modeled as solid surfaces. Although this is an unrealistic representation of the model, it is an effective means to determine the effect of the door recesses on torsional stiffness. To remain consistent, the same torsional stiffness model, loading conditions, laminate lay-up, and constraints were applied to the model as were applied to the preliminary model. Fig. 10 shows a suspension front end deflection of approximately 2.5 mm, yielding a torsional stiffness of 11798.4 Nm/deg, more

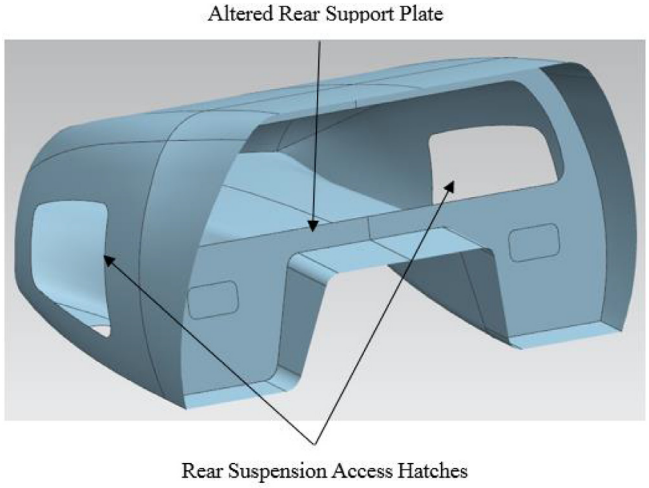

Fig. 9. Altered rear geometry.

than double the torsional stiffness of the preliminary model. This shows that the door recesses have a significant effect on the torsional stiffness.

A more realistic model was developed by reducing the size of the chassis door recesses from the preliminary model – see Fig. 11. Smaller recesses should improve the torsional stiffness value. In the present analysis, the doors are not considered structural elements due to their intended method of mounting.

Again, the finite element model set up remained unchanged as implemented in the previous models. Fig. 12 illustrates an approximate deflection of the front suspension ends of 4.159 mm, yielding a torsional stiffness value of 7092.2 Nm/deg. This is a significant increase in the torsional stiffness from the preliminary torsional stiffness result. It is interesting to note that a small geometry alteration resulted in a significant torsional stiffness increase from the preliminary model because such a minor geometry change did not significantly affect the mass, an increase of 2.1%, of the chassis resulted in a significant increase in the torsional stiffness, namely a 29.2% increase. The geometry alterations resulted in an estimated mass of 42.45 kg.

The effect of lay-up modifications was investigated next. To increase the torsional stiffness a honeycomb core, which exhibits far greater stiffness properties than foam, was investigated. An aluminum honeycomb was selected because of its superior physical properties. However, an aluminum honeycomb does not bend well in more than one direction and cannot be implemented at regions of high curvature. Therefore, a combination of foam and honeycomb cores was used to resolve the problem. The following illustrates the different regions of the chassis and their respective lay-ups:

- Roof and Sides – [0°; 45°; 5 mm Honeycomb Core; 45°; 0°]
- Suspension Mounts – [0°; 45°; 0°; 10 mm Foam Core; 0°; 45°; 0°]
- Inner Structure – [0°; 45°; 5 mm Honeycomb Core; 45°; 0°]
- Front and Rear – [45°; 3 mm Foam Core; 0°]
- Hood – [0°; 3 mm Honeycomb Core; 45°]

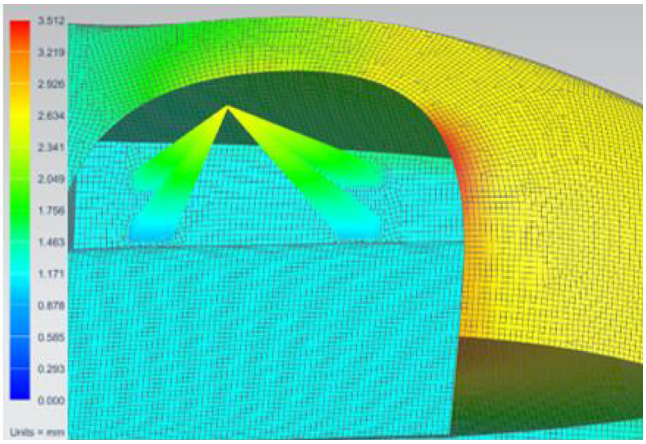

Fig. 10. Deflection result of chassis with enclosed doors.

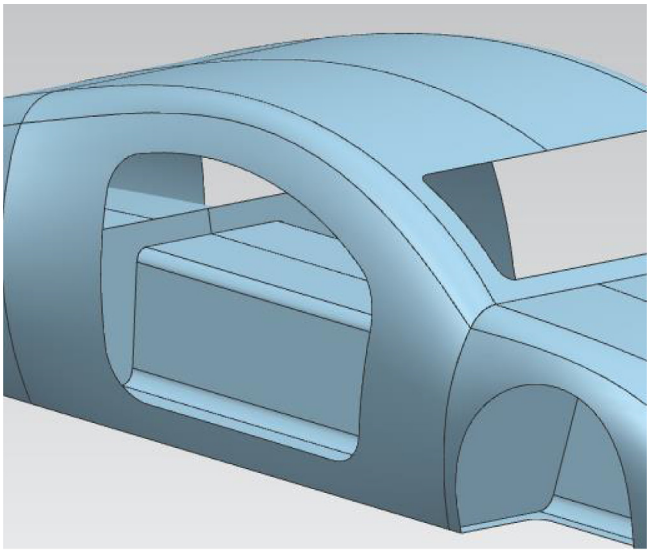

Fig. 11. Altered model with compact doors.

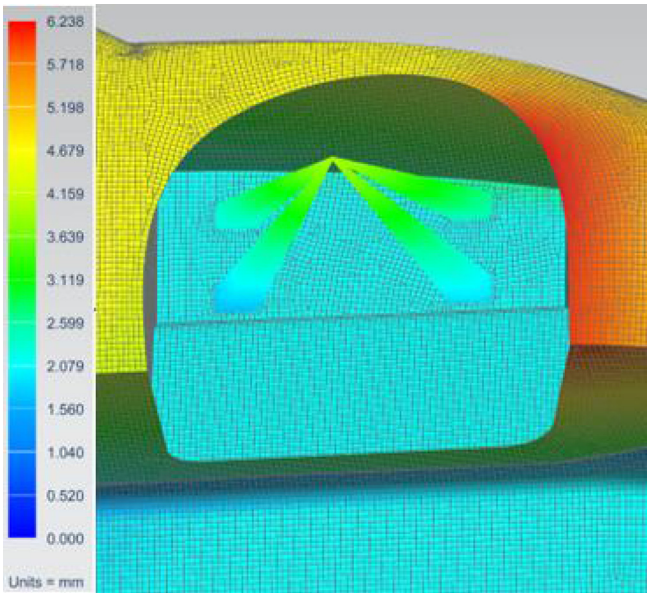

Fig. 12. Deflection result of chassis with compact doors.

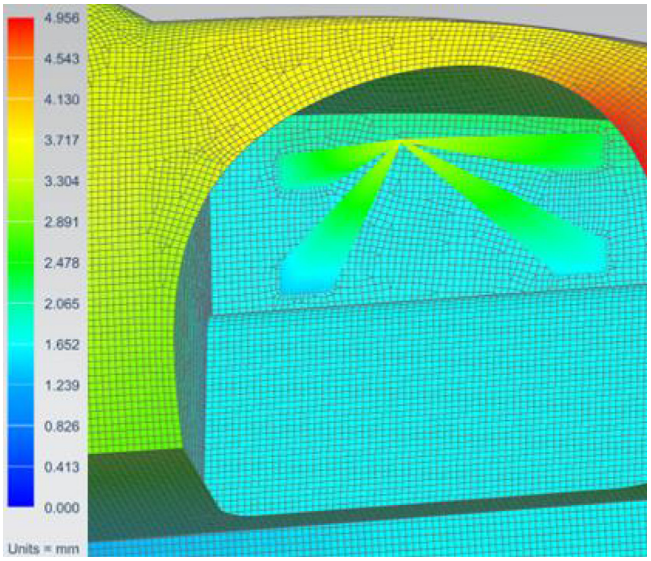

Fig. 13. Deflection result of composite honeycomb and foam cores.

The above laminate lay-ups were applied to the model with compact doors. The same torsional stiffness analysis, under the same loading conditions, was conducted, and a deflection of approximately 3.6 mm (see Fig. 13) was achieved. When substituted into the relevant equations, this yielded a torsional stiffness of 8193.4 Nm/deg which exceeds the failure criteria of 4000 Nm/deg, and results in a safety factor of 2.05 being present in the design.

It is evident that the aluminum honeycomb core has a significant effect on the torsional stiffness of the chassis. In addition to this, the estimated mass of the chassis decreased to 40.05 kg; a 5.6% decrease. This illustrates that a honeycomb core increases the stiffness of a chassis while reducing its weight when compared to a foam core.

To verify that the torsional stiffness parameter is the most important key performance indicator regarding chassis design, vertical bending and lateral bending load cases were simulated. The vertical bending analysis models the chassis as a simply supported beam with the rear suspension mounting locations modeled as pin supports, only allowing rotation about their own axis, and the front suspension mounting locations modeled as roller supports that only allows translation along the length of the chassis and rotation about its own axis. A vertical load, the magnitude of which the literature suggests is 1 g [17], is then applied to the chassis center and the maximum deflection, present at the mid-span, was determined. The simulation resulted in a maximum deflection of 5.275 mm – see Fig. 14. For the chassis to satisfy the vertical bending failure criteria, the chassis must not deflect more than 1/360th of the chassis length, which translates to a maximum allowable deflection of 12.29 mm. The maximum deflection is 57.1% below that of the maximum allowable deflection. This verifies that the satisfaction of the torsional stiffness failure criterion results in the satisfaction of the vertical bending failure criterion.

The torsional stiffness model has resulted in a suitable geometry and lay-up being generated, but it did not consider whether the material would be able to withstand the stresses present. This is verified if the structure satisfies the fiber fracture failure criterion. To determine this, the maximum normal stress induced in the structure has to be computed. There can be a vast number of planes passing through the given areas of a structure, each with its own normal stress value. There will be one plane on which the normal stress is maximal which corresponds to the maximum principal stress. Principal stresses are the components of the stress tensor when the basis is altered in such a way that the shear components become zero. This can be illustrated by the Mohr circle [44]. Maximum principal stress is particularly important to consider regarding composite materials where the direction of the stress is

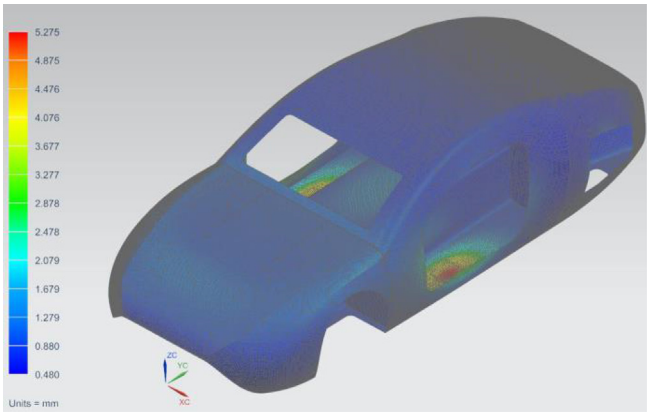

Fig. 14. Vertical bending model maximum deflection.

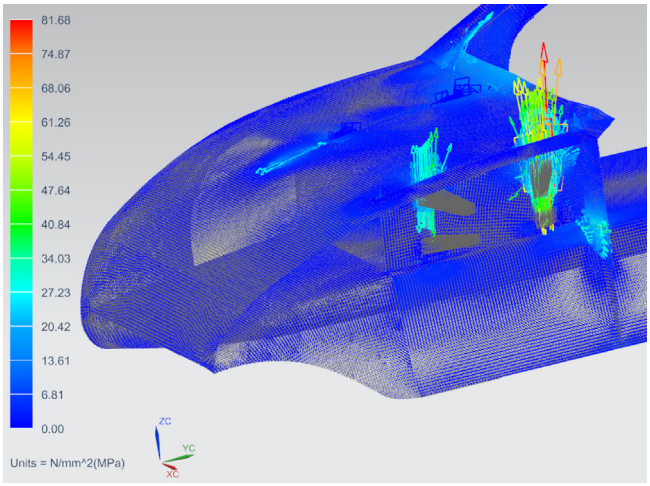

Fig. 15. Maximum principal stresses.

imperative for determining an appropriate laminate lay-up orientation. Fig. 15 illustrates a maximum principal stress of 81.68 MPa in the vertical direction. This is expected because the loads applied to the suspension mounts are vertical. The maximum principal stress is present at the front suspension mounts where 'hardpoints' would need to be constructed to account for stress concentrations. The maximum principal stress is concentrated at the front suspension mount. However, the maximum principal stress is still below that of the tensile strength of 464.4 MPa of the face material [41]. This shows that the chassis can withstand the stresses imparted to it by the suspension and would satisfy the fiber fracture failure mode criterion. According to the theory found in [45] the safety factor for the chassis, based on the maximum stress criteria, was calculated to be 5.69.

The maximum principal stress is the maximum stress state that the chassis is subjected to. This stress arises from the torsional stiffness model. To verify the significance of the torsional stiffness parameter, the maximum bending stress induced from a lateral bending model was compared to the maximum principal stress. A lateral bending model simulates the loads that the chassis is subjected to when cornering. To simulate this beam theory is used again, as with the vertical bending model. The loads are applied to the sides of the chassis, to simulate the forces that arise from the inertia of the chassis when cornering. The literature suggests that the maximum allowable lateral acceleration should not exceed 1 g [17] for a chassis to exhibit sufficient bending stiffness. This load is evenly distributed over the sides of the chassis in the same direction. The rear suspension mounts are modeled as a pin support, allowing vertical rotation perpendicular to their own axis, and the front suspension mounts are modeled as roller supports,

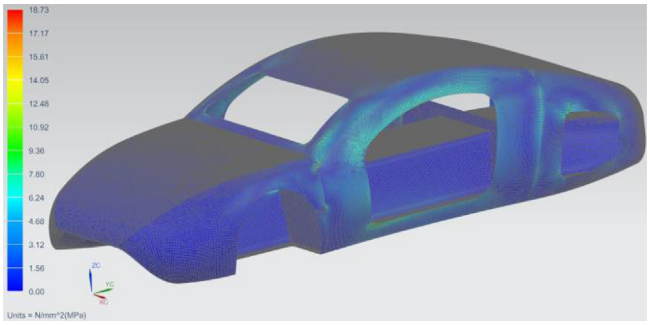

Fig. 16. Lateral bending model maximum stress.

allowing translation along the length of the chassis and vertical rotation. The bending stress result is analyzed and compared to the maximum principal stress. Fig. 16 illustrates a maximum bending stress of 18.73 MPa; 77.1% less than the maximum principal stress present in the chassis. This indicates that the torsional stiffness model results in higher stresses being exerted on the chassis, further signifying the importance of the torsional stiffness parameter.

8. Conclusion

This paper reported on the development of a structurally sound composite monocoque chassis through an iterative finite element analysis process. Regarding chassis design, one of the prominent key performance indicators is torsional stiffness. A preliminary model was developed and loaded according to the torsional stiffness model. The geometry and lay-up was modified with the intention of increasing the torsional stiffness. The geometry modifications included the addition of rear suspension access hatches, alteration of the rear support plate, and a reduction in size of the door recesses. The FEA illustrated that the chassis torsional stiffness was significantly dependent on the geometry and laminate lay-ups of a chassis. This is evident by the 29.2% increase in torsional stiffness by compacting the door recesses of the chassis. It is also important to note that an aluminum honeycomb offers a significant increase, namely 15.5%, on the torsional stiffness value, and a torsional stiffness of 8193.4 Nm/deg was attained. In conclusion, the chassis geometry, laminate layup and core material significantly affect the torsional stiffness. Table 1 gives a summary of the iterations and the corresponding torsional stiffness values.

Model	Torsional Stiffness (Nm/deg)
Preliminary	5489.8
Altered Rear Geometry and Compact Doors	7092.2
Composite Aluminum and Foam Core	8193.4

An analysis of the suspension mounting locations was conducted to ensure that the maximum principal stress does not exceed the maximum allowable stress of the reinforcement material. The analysis of the principal stresses yielded that the maximum principal stress, namely 81.68 MPa, resulting in a safety factor of 5.69, did not exceed the ultimate tensile strength of the face material. The analysis illustrated that the maximum principal stresses were applied vertically at the front suspension mounting points, indicating that the applied loads from the front suspension will be transmitted along the reinforcement material fibers.

Appendix A

Summary of loading conditions and constraints.

Loading Condition	Torsional Stiffness	Vertical Bending	Lateral Bending
Magnitude of Applied Load	3 g	1 g	1 g
Rear Suspension X-axis Translation	Fixed	Fixed	Fixed
Rear Suspension Y-axis Translation	Fixed	Fixed	Fixed
Rear Suspension Z-axis Translation	Fixed	Fixed	Fixed
Rear Suspension X-axis Rotation	Fixed	Free	Fixed
Rear Suspension Y-axis Rotation	Fixed	Fixed	Fixed
Rear Suspension Z-axis Rotation	Fixed	Fixed	Free
Front Suspension X-axis Translation	Free	Fixed	Fixed
Front Suspension Y-axis Translation	Free	Fixed	Fixed
Front Suspension Z-axis Translation	Free	Fixed	Fixed
Front Suspension X-axis Rotation	Fixed	Free	Fixed
Front Suspension Y-axis Rotation	Free	Fixed	Fixed
Front Suspension Z-axis Rotation	Fixed	Fixed	Free

Appendix B

Table of simulation material properties [41].

Material	AMT 2 × 2 Twill Weave	M60 Cell Foam Core	PCF Aluminum Core
Young's modulus (E1)	47000 MPa	44 MPa	6.9 MPa
Young's modulus (E2)	47000 MPa	44 MPa	6.9 MPa
Young's modulus (E3)	N/A	N/A	1241.6 MPa
Density	1600 kg/m^3	65 kg/m^3	4919 kg/m^3
Poisson's ratio (NU)	0.05	0.3	0.1
Poisson's ratio (NU13)	N/A	N/A	0.1
Poisson's ratio (NU23)	N/A	N/A	0.1
Shear modulus (G)	5100 MPa	20 MPa	186.2 MPa
Shear modulus (G13)	N/A	N/A	469 MPa

References

[1] E. Betancur, R. Mejia-Gutierrez, G. Osorio-Gomez, A. Arbelaez, Design of structural parts for a racing solar car, in: International Joint Conference on Mechanics, Design Engineering and Advanced Manufacturing, Catania, 2016.
[2] C.A. Eurenius, N. Danielsson, A. Khokar, E. Krane, M. Olofsson, J. Wass, Analysis of Composite Chassis, Chalmers University of Technology, Göteborg, 2013.
[3] G. Genta, L. Morello, The Automotive Chassis, Springer, Torino, 2009.
[4] Bridgestone World Solar Challenge, Bridgestone World Solar Challenge 2017 Regulations, Bridgestone World Solar Challenge, 2016.
[5] W.S. Hurter, N.J. Van Rensburg, D.M. Madyira, G.A. Oosthuizen, Static analysis of advanced composites for the optimal design of an experimental lightweight solar vehicle suspension system, in: ASME 2014 International Mechanical Engineering Congress & Exposition, Montreal, 2014.
[6] M. Mohsan, Front and Rear Suspension Design for Solar Car, University of Malaysia Pahang, Pekan, 2016.
[7] F.V. De Camargo, C. Fragassa, A. Pavlovic, M. Martignani, Analysis of the suspension design evolution in solar cars, FME Trans. 45 (3) (2017) 394–404.
[8] Solar Team Nuon, Nuon's Foundation: The Suspension, 2017. [Online]. Available: <https://www.nuonsolarteam.nl/nuna/>. (accessed 28.02.18).
[9] A. Goerge, W. Riley, Design, Analysis and Testing of a Formula SAE Car Chassis SAE Technical Paper, Cornell University, New York, 2002.
[10] A. Crocombe, E. Sampe, A. Somiotti, Chassis Torsional Stiffness: Analysis of the Influence on Vehicle Dynamics, in: SAE 2010 World Congress & Exhibition, Detroit, Michigan, USA, 2010.
[11] G. Davies, Materials for Automobile Bodies, Elsevier, Oxford, 2012.
[12] G. Minak, C. Fragassa, F.V. de Camargo, A Brief Review on Determinant Aspects in Energy Efficient Solar Car Design and Manufacturing, in: Sustainable Design and Manufacturing, Cham, Switzerland, 2017.
[13] J. Wanberg, Composite Materials Fabrication Handbook, Wolfgang Publications, Stillwater MN, 2009.
[14] S. Paterson, P. Vijayaratnam, C. Perera, G. Doig, Design and development of the Sunswift eVe solar vehicle: a record-breaking electric car, J. Automobile Eng. 230 (14) (2016) 1972–1986.
[15] D. Mathijsen, Redefining the motor car, Reinf. Plast. 60 (2016) 154–159.
[16] S. Tamura, Teijin advanced carbon fiber technology used to build solar car for world solar challenge, Reinf. Plast. 60 (2016) 160–163.
[17] D.R. Carrol, The Winning Solar Car, SAE International, Warrendale, PA, 2003.
[18] E.J. Barbero, Introduction to Composite Materials Design, Taylor and Francis Group, London, 2011.
[19] M.F. Ashby, Materials Selection in Mechanical Design, Butterworth-Heinemann, Oxford, 2005.
[20] P.K. Mallick, Composites Engineering Handbook, Marcel Dekker Inc., Michigan, 1997.
[21] O.T. Thomsen, E. Bozhevolnaya, A. Lyckegaard, Sandwich Structures 7: advancing with Sandwich Structures and Materials, in: 7th International Conference on Sandwich Structures, Aalborg, 2005.
[22] P.P. Camanho, Failure Criteria for Carbon-Reinforced Polymer Composites, University of Porto, Faculty of Engineering, Porto, 2002.
[23] S.W. Tsai, E.M. Wu, A general theory of strength for anisotropic materials, J. Compos. Mater. 5 (1) (1971) 58–80.
[24] H.D. Velie, Chassis Torsional Rigidity Analysis for a Formula SAE Racecar, University of Michigan, Department of Mechanical Engineering, Ann Arbor, 2016.
[25] R. Abrams, Formula SAE Racecar Analysis: Simulation & Testing of the Engine as a Structural Member, The University of Western Ontario, Ontario, 2008.
[26] D. Milliken, W. Milliken, Race Car Vehicle Dynamics, SAE International, 1995.
[27] L. Jiang, G. Wang, G. Gong, R. Zhang, Lightweight Design of a FSC Car Based on Modal and Stiffness Analysis, in: FISITA 2012 World Automobile Congress, Beijing, 2012.
[28] R. Hibbeler, Mechanics of Materials, first ed., Pearson Prentice Hall, Upper Saddle River, USA, 2008.
[29] E. Law, S. Raju, L. Thompson, Design of a Winston Cup Chassis for Torsional Stiffness, in: Motorsports Engineering Conference and Exposition, Dearborn, Michigan, USA, 1998.
[30] A. Goerge, Y. Tai, O.A. Badu, J. Wu, Design, Analysis, and Simulation of an Automotive Carbon Fiber Monocoque Chassis, Cornell University, Ithaca, 2014.
[31] M. Hagan, J. Rappolt, J. Waldrop, Formula SAE Hybrid Carbon Fibre Monocoque/Steel Tube Frame Chassis, California Polytechnic State University, San Luis Obispo, 2014.
[32] N.Y. Reddy, V.S. Kumar, Study of different parameters on the chassis space frame for the sports car by using FEA, IQSR J. Mech. Civ. Eng. 9 (1) (2013) 1–2.
[33] Siemens, Siemens PLM Software, Siemens, 2017. [Online]. Available: <https://www.plm.automation.siemens.com/en_us/products/simcenter/nastran/>. (accessed 28.04.17).
[34] S. Heimbs, S. Heller, P. Middendorf, F. Hähnel, J. Weiße, Low velocity impact on CFRP plates with compressive preload: test and modelling, Int. J. Impact Eng. 36 (10–11) (2009) 1182–1193.
[35] Q. Liu, Y. Lin, Z. Zong, G. Sun, Q. Li, Lightweight design ofcarbon twill weave fabric composite body structure for electric vehicle, Compos. Struct. 97 (2013) 231–238.
[36] A. Jain, Computational Analysis and Optimisation of Torsional Stiffness of a Formula-SAE Chassis, in: SAE 2014 World Congress & Exhibition, 2014.
[37] M. Broad, T. Gilbert, Design, Development and Analysis of the NCSHFH 09 Chassis SAE Technical Paper, North Carolina State University, Raleigh, 2009.
[38] J.Y. Wong, Theory of Ground Vehicles, John Wiley and Sons Inc., New York, 2001.
[39] T. Bartlett Quimby, A Beginner's guide to the Steel Consrtuction Manual, 2011. [Online]. Available: <http://www.bgstructuralengineering.com/BGSCM14/Contents.htm>. (accessed 20.05.18).
[40] S. Rugdeo, S. Singh, N. Witteveen, M. Woods, P. Sinclair, D. Raghubeer, UKZN Solar Car: Second Semester Report, University of KwaZulu-Natal, Durban, 2014.
[41] AMT Composites, amt composites, 2017. [Online]. Available: <http://www.amtcomposites.co.za/products>. (accessed 25.01.17).
[42] E. Borjesson, Layered solid-shell Elements for Accurate Prediction of Stresses in Laminate Composites, Chalmers University of Technology, Goteborg, 2016.
[43] J. Denny, S. Govender, B. Ngema, J. Moodley, UKZN Solar Car: 1st Semester Report, University of KwaZulu-Natal, Durban, 2015.
[44] J.M. Gere, B.J. Goodno, Mechanics of Materials, Global Engineering, Stanford, 2013.
[45] D. Gay, Composite Materials: Design and Applications, CRC Press Taylor & Francis Group, Boca Raton, 2015.